Excitons and nonlinear optical spectra in conjugated polymers

S. Abe

Electrotechnical Laboratory, Umezono, Tsukuba 305, Japan
and Institut für Physikalische Chemie, Johannes-Gutenberg-Universität, D-6500 Mainz,
Federal Republic of Germany

M. Schreiber

Institut für Physikalische Chemie, Johannes-Gutenberg-Universität, D-6500 Mainz, Federal Republic of Germany

W. P. Su and J. Yu

Department of Physics, University of Houston, Houston, Texas 77204-5504
(Received 16 January 1992)

Excitons in conjugated polymers are studied theoretically in the Su-Schrieffer-Heeger model supplemented by long-range Coulomb interactions. The relationship between exciton energies and basic interaction parameters is clarified. Linear and third-order nonlinear optical susceptibilities (two-photon absorption, electroabsorption, and third-harmonic generation) have been calculated, elucidating the significance of singlet and triplet excitons and unbound electron-hole pairs. Using only moderate interaction strength, various experiments in polydiacetylene can be interpreted in a consistent way.

Recently there has been an increasing interest in the nonlinear optical properties of excitons confined in low-dimensional geometries, e.g., quantum wells and quantum wires of inorganic semiconductors. Other well-known examples are conjugated polymers, which are in a sense ideal one-dimensional (1D) semiconductors.[1,2] The significance of excitons in conjugated polymers has been recognized for some time in a class of materials known as polydiacetylene (PDA).[2,3] Yet most of the theoretical studies of the nonlinear optical properties of conjugated polymers in the literature were limited to either independent-electron models[4-6] or strong-correlation models for very short chains.[7] Here we report calculations of third-order nonlinear optical susceptibilities $\chi^{(3)}$ for long chains in a model which takes account of exciton formation. We also report results on triplet excitons.

Initial calculations of exciton states in conjugated polymers demonstrated that the exciton has an intermediate character between Frenkel and Wannier exciton.[8] This can be understood as a characteristic feature of 1D Wannier excitons in Peierls semiconductors.[9] The special nature of the 1D excitons manifests itself also as unusually large optical transition dipole moments.[9] Therefore it is natural to expect the excitons to play important roles in $\chi^{(3)}$.

To study excitons in conjugated polymers, we consider the one-electron tight-binding Hamiltonian of the Su-Schrieffer-Heeger model[10]

$$H_0 = -\sum_{n,s} t_{n+1,n}(C^\dagger_{n+1,s}C_{n,s} + C^\dagger_{n,s}C_{n+1,s}) \quad (1)$$

perturbed by the electron-electron interaction terms

$$H_{e-e} = \sum_n V_{n,n}\rho_{n\uparrow}\rho_{n\downarrow} + \frac{1}{2}\sum_{n,m(\neq n)}\sum_{s,s'} V_{n,m}\rho_{n,s}\rho_{m,s'} . \quad (2)$$

Here $C^\dagger_{n,s}$ creates an electron at site n with spin s and $\rho_{n,s} \equiv C^\dagger_{n,s}C_{n,s} - \frac{1}{2}$, where $-\frac{1}{2}$ ensures charge neutrality. The nearest-neighbor transfer energies $t_{n+1,n}$ depend on the bond lengths. Since we do not consider electron-phonon coupling in the present paper, we assume that the system is already Peierls distorted with $t_{n+1,n} = t + (-1)^n\delta t$, as in polyacetylene. Although it is straightforward to include an additional modulation with the period of four atoms in PDA, we use here the simpler dimerized system so that the model has as few parameters as possible yet contains the essential physics. For the interaction terms in Eq. (2) we use a long-range potential $V_{n,m} = V/|n-m|$ (for $n\neq m$) and the on-site Coulomb energy $V_{n,n} = U$. We can write $V = e^2/\epsilon a$, where e, ϵ, and a are the electron charge, the dielectric constant, and the average interatomic spacing, respectively. For example, $\epsilon \approx 5$ and $a \approx 1.4$ Å correspond to $V \approx 2$ eV.

The calculation procedure is a standard one.[11] We first obtain the ground state of the one-electron Hamiltonian H_0, and construct the excited states of a single electron-hole (e-h) pair from the ground state. Then the matrix of the total Hamiltonian within the single-excitation subspace is diagonalized. Actual calculations have been carried out numerically for a ring of N sites (up to $N = 800$). The excited states are classified by the total wave number K, the total spin of the e-h pair (singlet or triplet), and the symmetry of the wave function of the relative motion of electron and hole: symmetric (A_g) or antisymmetric (B_u) with respect to the spatial inversion at a bond center.

The energy levels thus obtained at $K=0$ are plotted as functions of V in Fig. 1, with U assumed to scale as $U = 2V$. Exciton states split off from the (quasi)continuum of the unbound e-h states upon increasing V, while the gap E_c of the e-h continuum grows
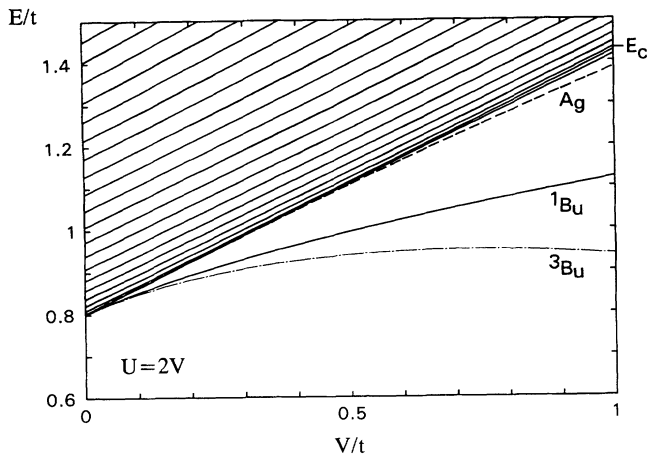
FIG. 1. Energy levels vs the interaction strength V for $U = 2V$, $\delta t = 0.2t$, and $N = 400$. In addition to the lowest ^1B_u, ^3B_u, and A_g (singlet and triplet degenerate) states, only higher ^1B_u states are shown to avoid confusion. E_c indicates the edge of the electron-hole continuum for $V = t$.

linearly with V due to first-order energy correction of the one-electron states.[12] The lowest singlet and triplet excitons are of B_u symmetry and have fairly large binding energies even for small V. The next exciton state with A_g symmetry (singlet and triplet degenerate) is identifiable in the region $V \gtrsim 0.5t$ for the system size used. We see some more exciton states just below E_c for $V \sim t$, but the sizes of these excitons are comparable to the system size, so that we do not distinguish them from the e-h continuum.

Figure 2 shows the dependence of the states on U for fixed V. The energies of the lowest singlet and triplet B_u excitons strongly depend on U, while the other states and the continuum edge E_c are insensitive to U. Physically, we expect $U/V \gtrsim 1$. The triplet energy is higher than the singlet energy for $U \approx V$, while the order is reversed for much larger U. The crossing occurs at $U/V \cong 1.39$. (It can be shown[13] that this value is independent of the other
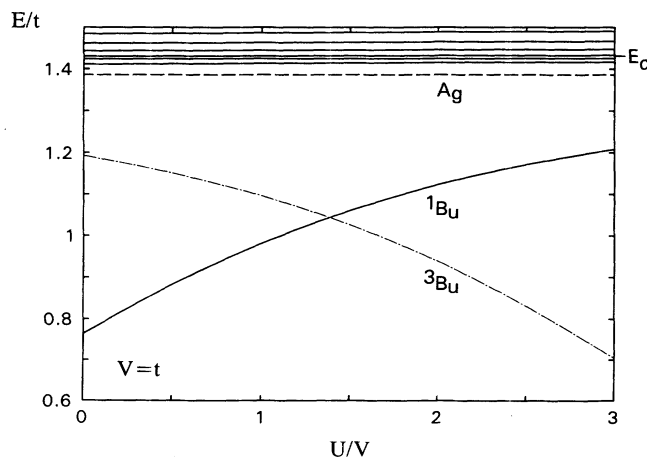

FIG. 2. Energy levels vs the ratio U/V for $V = t$, $\delta t = 0.2t$, and $N = 400$.

parameters.) Note that the ratio of the binding energies of singlet and triplet excitons is almost uniquely related to the ratio U/V in the present model.

Experimentally, the existence of the relaxed triplet state with a "binding energy" of ~ 1.4 eV has been reported in PDA crystals.[14] It is considered to be an exciton-polaron (neutral bipolaron), so that the binding energy contains the energy gain of the polaron formation. The latter has previously been calculated as ~ 0.5 eV.[15] Therefore, the purely electronic binding energy of the lowest triplet exciton is estimated as ~ 0.9 eV.[16] On the other hand, we will see below that the binding energy of the lowest singlet B_u exciton is ~ 0.6 eV. The ratio of these two energies corresponds to $U/V \approx 2$ in the present model (see Fig. 2).

We have calculated the linear susceptibility $\chi^{(1)}$ and third-order nonlinear susceptibilities $\chi^{(3)}$ by using the standard formulas by Orr and Ward.[17] Matrix elements between ground and excited states and among excited states have been calculated for the dipole $-e\sum_n x_n C_n^\dagger C_n$, where x_n is the position of the site n. A constant imaginary energy (lifetime broadening) Γ is assumed for all the excited states. In the following we show results for $\delta t = 0.2t$, $V = t$, and $U = 2V$. These values turn out to give approximately correct exciton energies in PDA.

We briefly comment on the magnitudes of the calculated susceptibilities. We have checked that they increase linearly with chain length N for large N. In the case of $\chi^{(3)}$ for third-harmonic generation (THG) a strong power-law dependence on N remains up to moderately long $(N \approx 100)$ chains, in a similar manner as in an independent-electron model.[6] The size of $N = 800$ used here is large enough to obtain the bulk susceptibilities. We define $\chi_0^{(1)} \equiv \sigma e^2 a /t$ and $\chi_0^{(3)} \equiv \sigma e^4 a^3 /t^3$ per unit volume, where σ is the density of chains per unit area. Typical parameter values like $a \approx 1.4$ Å, $\sigma \approx 10^{14}$ cm^{-2}, and $t \approx 2$ eV for PDA give $\chi_0^{(1)} \approx 0.1$ and $\chi_0^{(3)} \approx 4 \times 10^{-13}$ esu. With these values the susceptibilities presented below reproduce correct orders of magnitude compared with experiments. For a quantitative agreement, local-field corrections[6] have to be taken into account.

Figure 3 shows the linear one-photon absorption spectrum $-\mathrm{Im}\chi^{(1)}(\omega)$. Due to the selection rule in this case only ^1B_u states are optically allowed. The spectrum is dominated by the peak at E_1, corresponding to the energy of the ^1B_u exciton. It shows also very weak absorption above about E_c due to the e-h continuum. The results are consistent with calculations in a continuum model.[9] Experimentally, absorption spectra of PDA are characterized by a strong peak at about 2 eV with phonon sidebands extending above this.[3] The peak can be ascribed to the B_u exciton peak at E_1 in Fig. 3 with $t \approx 2$ eV, while the tail of the sidebands masks the calculated weak absorption above E_c.

Figure 4 displays the two-photon absorption (TPA) spectrum $-\mathrm{Im}\chi^{(3)}(-\omega;\omega,-\omega,\omega)$. There is no structure at the energy E_1, since the selection rule for TPA allows only ^1A_g states. Naturally the peak is located at the respective energy E_2. In contrast to the one-photon absorption in Fig. 3, the e-h continuum contributes to the TPA significantly, forming a large tail on the high-energy
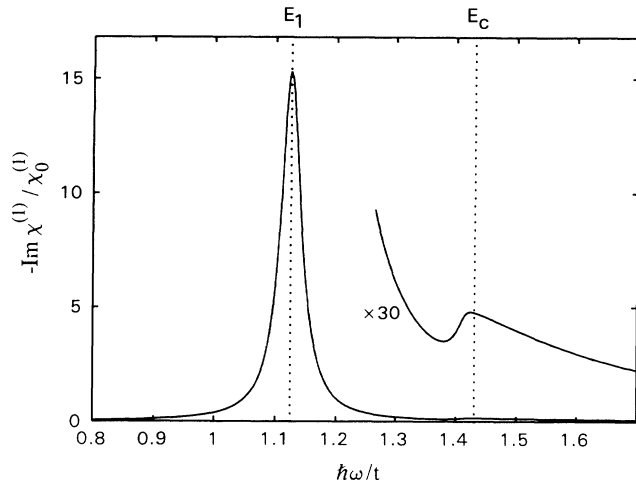
FIG. 3. Linear absorption spectrum for $V=t$, $U=2V$, $\delta t =0.2t$, $N =800$, and $\Gamma =0.02t$. E_1 denotes the energy of the lowest ^1B_u exciton and E_c the edge of the electron-hole continuum. $\chi_0^{(1)}$ is the characteristic linear susceptibility (see text).
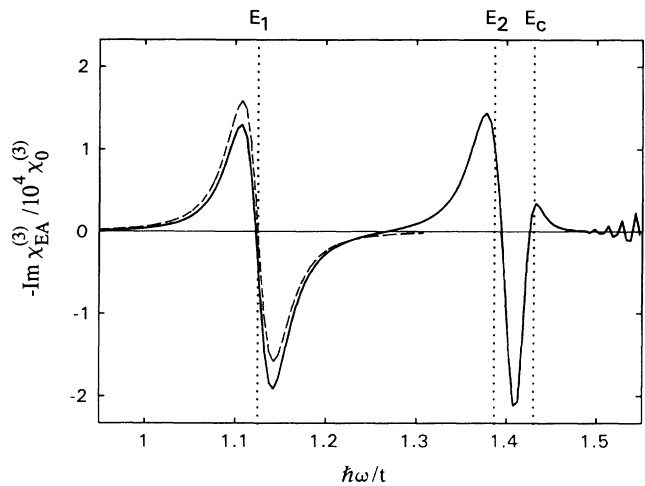
FIG. 5. Electroabsorption spectrum for the same parameters as in Figs. 3 and 4, except $\Gamma =0.03t$. The broken curve is the first derivative of the corresponding linear absorption spectrum (in arbitrary units). The oscillation above $\hbar\omega \approx 1.5t$ is a finite-size effect.

side of the peak, as E_c is close to E_2. The results are consistent with a calculation in the continuum model.[18]

Three-wave mixing experiments in PDA solutions[19] have revealed the existence of a two-photon absorbing A_g state in the energy region of $1.2E_1 \sim 1.6E_1$ in agreement with Fig. 4 (the exact energy is obscured by large broadening). Recent TPA experiments in PDA films also have shown similar behavior.[20]

In Fig. 5 we present the electroabsorption (EA) spectrum $-\mathrm{Im}\chi^{(3)}(-\omega;\omega,0,0)$. The low-energy structure near E_1 is approximately proportional to the first derivative of the linear absorption, corresponding to a redshift (Stark shift) of the B_u exciton peak under the electric field. The high-energy structure is similar to the theoretical spectrum of an electric-field-modulated interband ab-

sorption edge in 1D,[21] but with an important difference: the positive part near E_2 in Fig. 5 is much stronger than expected from Fig. 3 of Ref. 21. Actually, this peak is mainly due to the A_g exciton at E_2, which becomes allowed under the electric field. The two contributions from the band-edge effect and the exciton effect are both important as long as the binding energy of the A_g exciton is comparable to the broadening Γ.

Figure 5 is in excellent agreement with experiments in PDA crystals[22,23] (besides phonon sidebands) if we choose $t \approx 2$ eV, so that $E_c -E_1 \approx 0.6$ eV. Most importantly, our result unites the contrasting explanations of the high-energy structure as a band-edge effect[22] or an exciton effect.[23]

Figure 6 displays the THG intensity $|\chi^{(3)}(-3\omega;\omega,\omega,\omega)|$. The two low-energy peaks are due
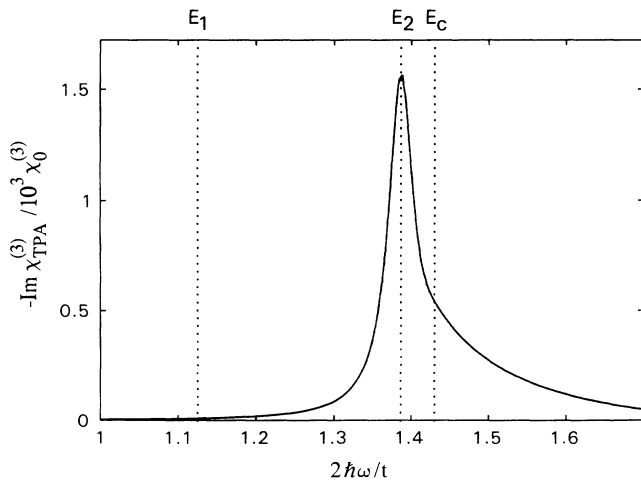
FIG. 4. Two-photon absorption spectrum for the same parameters as in Fig. 3. E_2 is the energy of the lowest ^1A_g exciton, and $\chi_0^{(3)}$ is the characteristic third-order susceptibility (see text).
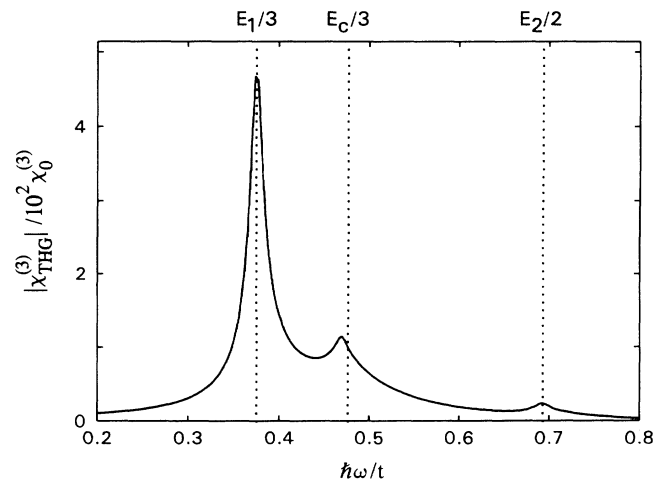
FIG. 6. Third-harmonic generation spectrum for the same parameters as in Figs. 3 and 4.

to the three-photon resonances to the ^1B_u exciton and to the e-h continuum. Although the states allowed for the three-photon resonances are the same as for the linear absorption, the peak near $E_c/3$ in Fig. 6 is much larger than the corresponding peak near E_c in Fig. 3. The high-energy peak at $E_2/2$ in Fig. 6 is due to the two-photon resonance to the ^1A_g exciton. It is weak, as in the case of noninteracting electrons.[5,6]

The recently observed THG spectrum of an oriented PDA film[24] is well reproduced by the two main peaks in Fig. 6 (cf. Fig. 2 of Ref. 24). The EA spectrum[25] of the same sample is also reproduced by our model (Fig. 5) with the same parameters. In contrast the second peak in the THG spectrum of a PDA Langmuir-Blodgett multi-layer[26] has been interpreted not as a three-photon resonance to E_c but as a two-photon resonance to an A_g state below E_1.[26] Such a state is well known for polyene oligo-mers[27] and arises from an intricate admixture of double excitations. But for the bulk materials studied here the respective state should correspond to spin-wave-like excitations of an infinite chain, not contributing to the nonlinear optical properties at all. Accordingly, no respective structures can be found in EA measurements.[23-25]

In conclusion, we demonstrated that experiments on triplet states, linear absorption, TPA, EA, and THG in PDA can be interpreted consistently within the present approach which, although comprising a conventional model and a standard calculational procedure, had not been applied to these or similar materials. We note that for the description of the spectra, a chain length of at least 100 sites is necessary to obtain the bulk properties. Agreement between theory and experiment was achieved by assuming $V \approx t \approx 2$ eV and $U \approx 4$ eV.[28]

For other polymers like polythiophenes and polysilanes we expect our model to yield correct spectra if the parameters are appropriately chosen. Preliminary results for polysilanes show agreement with TPA,[29] EA,[30] and THG (Ref. 31) experiments. Based on the present work, the study of exciton polarons, the consideration of disorder effects, and the quantitative description of nonlinear spectra of various one-dimensional systems (e.g., semiconductor quantum wires) will be the subject of further work.

[1]C. Sauteret et al., Phys. Rev. Lett. **36**, 956 (1976).
[2]B. I. Green, J. Orenstein, and S. Schmitt-Rink, Science **247**, 679 (1990).
[3]D. Bloor et al., Chem. Phys. Lett. **24**, 407 (1974).
[4]G. P. Agrawal, C. Cojan, and C. Flytzanis, Phys. Rev. B **17**, 776 (1978).
[5]W. K. Wu, Phys. Rev. Lett. **61**, 1119 (1988).
[6]J. Yu et al., Phys. Rev. B **39**, 12 814 (1989).
[7]J. R. Heflin et al., Phys. Rev. B **38**, 1573 (1988); P. C. M. McWilliams, G. W. Haydon, and Z. G. Soos, ibid. **43**, 9777 (1991).
[8]M. R. Philpott, Chem. Phys. Lett. **50**, 18 (1977); D. R. Yarko-ny, Chem. Phys. **33**, 171 (1978); S. Suhai, Phys. Rev. B **29**, 4570 (1984).
[9]S. Abe, J. Phys. Soc. Jpn. **58**, 62 (1989).
[10]W. P. Su, J. R. Schrieffer, and A. J. Heeger, Phys. Rev. Lett. **42**, 1698 (1979).
[11]R. S. Knox, Theory of Excitons (Academic, New York, 1963).
[12]W. K. Wu and S. Kivelson, Phys. Rev. B **33**, 8546 (1986).
[13]S. Abe, J. Yu, and W. P. Su, Phys. Rev. B **45**, 8264 (1992).
[14]J. Orenstein, S. Etemad, and G. L. Baker, J. Phys. C **17**, L297 (1984); T. Hattori, W. Hayes, and D. Bloor, ibid. **17**, L881 (1984); L. Robins, J. Orenstein, and R. Superfine, Phys. Rev. Lett. **56**, 1850 (1986); M. Winter et al., Chem. Phys. Lett. **133**, 482 (1987).

[15]W. P. Su, Phys. Rev. B **36**, 6040 (1987).
[16]This argument implicitly assumes that the polaron size obtained in Ref. 15 is not smaller than the exciton size obtained in the present study. We have checked this.
[17]B. J. Orr and J. F. Ward, Mol. Phys. **20**, 513 (1971).
[18]S. Abe and W. P. Su, Mol. Cryst. Liq. Cryst. **194**, 357 (1991).
[19]R. R. Chance et al., Phys. Rev. B **22**, 3540 (1980).
[20]P. D. Townsend et al., Chem. Phys. Lett. **180**, 485 (1991).
[21]D. E. Aspnes and J. E. Rowe, Phys. Rev. B **5**, 4022 (1972).
[22]L. Sebastian and G. Weiser, Phys. Rev. Lett. **46**, 1156 (1981).
[23]Y. Tokura et al., J. Chem. Phys. **85**, 99 (1986).
[24]T. Kanetake et al., Appl. Phys. Lett. **54**, 2287 (1989).
[25]T. Hasegawa et al., Chem. Phys. Lett. **171**, 239 (1990); Synth. Metals **43**, 3151 (1991).
[26]F. Kajzar and J. Messier, Thin Solid Films **132**, 11 (1985).
[27]B. Hudson and B. Kohler, Synth. Metals **9**, 241 (1984).
[28]These values are much smaller than those commonly used in the strong-correlation models (Ref. 7), namely, $U \approx 11$ eV and $V \approx 8$ eV of the Ohno potential. This fact indicates the importance of screening in condensed phases and partly justifies the perturbative approach used in the present theory.
[29]Y. Moritomo et al., Phys. Rev. B **43**, 14 746 (1991).
[30]H. Tachibana et al., Solid State Commun. **75**, 5 (1990).
[31]Y. Iwasa et al., Synth. Metals (to be published).